RESEARCH ARTICLE

Stacked Ensemble Deep Learning for Outdoor Insulator Surface Condition Classification: A Profound Study on Water Droplets

ARAILYM SERIKBAY, (Graduate Student Member, IEEE),
MEHDI BAGHERI, (Senior Member, IEEE), AND AMIN ZOLLANVARI, (Senior Member, IEEE)
Electrical and Computer Engineering Department, School of Engineering and Digital Sciences, Nazarbayev University, Astana 010000, Kazakhstan

Corresponding author: Mehdi Bagheri (mehdi.bagheri@nu.edu.kz)

ABSTRACT Insulators are vital protection and isolation barriers used in power transmission systems. To prevent unexpected failures caused by severe weather conditions, it is important to develop intelligent insulator fault prognosis systems. To this end, this study has focused to examine and analyze normal (clean) and contaminated (wet) insulators through a new technique that can act as a catalyst for possible future solutions to the data-driven classification of insulator surface conditions. In particular, a novel stacked ensemble learning based on six pretrained deep convolutional neural networks (CNNs), which are used as level-0 generalizers in the stacked structure, is proposed. As the level-1 generalizer that is used in the stacked structure, a majority vote is considered among selected subsets of level-0 generalizers. In other words, training the level-1 generalizer is equivalent to selecting the best subset of pretrained CNNs for classifying a clean insulator surface from those sprayed with water droplets. Since a wetted insulator surface can enhance the electric field intensity and may lead to flashover when combined with other contaminants (dust, soil, cement, etc.), water droplets are considered a type of contamination in our study. Considering a tradeoff between performance and model complexity in training the level-1 generalizer points to two combinations of pretrained CNNs, namely, EfficientNetB2-ResNet50-Xception, and MobileNet-DenseNet121-Xception. Our empirical results show that (i) both combinations lead to better performance when compared with individual pretrained models, and (ii) the latter combination leads to a considerably lower complexity (∼39% less parameters) at the expense of ∼9% reduction in accuracy.

I. INTRODUCTION

Insulator surface corruption followed by leakage current flow leads to complications in electrical energy supply company operation. Even a single operating insulator outage may create a significant financial loss. Therefore, it is necessary to take alleviating actions to increase power distribution and transmission work efficiency. Researchers have conducted encouraging investigations regarding contaminated

The associate editor coordinating the review of this manuscript and approving it for publication was Ruisheng Diao.

insulator condition analysis using different approaches such as coating [1], [2], [3], [4], [39], [40], creepage distance extension [5], and washing [6]. The most used preventive action is covering the insulator surface with hydrophobic material, the so-called insulation protective coating. This silicone coverage inhibits the creation of conducting sheets. Consequently, the likelihood of possible breakdown and leakage current level is reduced [2]. Recently, a novel nano-room temperature vulcanizing (RTV) coating method was proposed to improve outdoor insulator functioning as a potential option for traditional coatings. Conjoining the nanoparticles

and polymer matrix can cause modifications in the insulator surface coating structure. Several investigations have evaluated the condition of high-voltage (HV) insulators using this technique [3], [4].

In [3], a clean fog artificial test with a nano-RTV coating was applied to determine the correlation between the flashover voltage level and porcelain insulator pollution severity. The results show the possibility of the nano-RTV-coated insulators increasing their functioning time in polluted regions. In [4], a superhydrophobic nanocoating test, which lasted for two years, was compared with nano-RTV and noncoated HV glass insulators. The results showed the efficiency of the proposed method only during the first few months after installation. However, the choice of the most desirable period for insulator coating, installation, and replacement is currently the subject of further investigation. The second possible suppressing action is escalating the existing insulator creepage distance, which leads to upward and downward trends in the leakage current and flashover voltage values, respectively [5]. However, the indicated technique is expensive and usually used when alternative measures are inapplicable. A frequently used third preventive action is insulator surface cleansing operations. Systematic insulator washing operations have proven to be notably efficient [6]. However, the main limiting factors are the optimal washing time (based on intermittent pollution levels) selection and its overpriced maintenance.

The insulator pollution severity measurement is the equivalent salt deposit density (ESDD) [7]. The proper inspection of the insulator pollution level gives necessary data for power utilities to correctly arrange cleansing or other maintenance actions. In turn, the indicated measurements lead to advancements in power transmission systems and avoidance of anticipated destructive outbreaks. Its surface contamination severity plays a critical role in power distribution over long distances and has different standards [8], [9], [10]. Current investigations have shown the insulator surface pollution severity and its considerable influence on the electrical and mechanical characteristics of insulators. In [11], a multilayer neural network based on the linear algebraic features of fifty-one insulator images was constructed to predict ESDD values related to different contamination levels. The flashover voltage and ESDD values are measured using a porcelain insulator and a digital camera. Another study shows that aggravation of the insulator contamination level is discriminated more clearly by spatial electric field variation features compared to the current flowing through the contaminated insulator surface [12]. A considerable amount of work has examined the ageing rate of porcelain insulators. Mechanical and electrical properties have investigated the proportion of silica, aluminium, and ferric oxides using microstructural analysis and showed the insulator materials' dependence on their internal features, service conditions, and operation procedure [13]. Huang et al. investigated the process of ice accretion on insulator surfaces based on different parameters,

such as temperature, wind velocity, water droplet volume, and its content [14]. The icing research executes and compares the results of simulation and artificial climate chamber methods, but practical validation tests should be completed before real-life implementation.

In recent years, the vulnerability of power transmission lines to different weather conditions has become increasingly evident [15], [16], [17], [18], [19], [20], [21], [22], [23], [24], [25], [26]. The Texas ice storm blackout in 2021 and the Italian power outage in 2013 are a few examples of how rain, ice, and wetting can lead to significant faults in high-voltage insulators, ultimately resulting in widespread power disruptions and economic losses. In only Texas, 10 million people were left without electricity and $130 billion was lost [26].

When mist or rain comes into contact with an insulator, its hydrophobic nature leads to the formation of water droplets on the surface. Several studies have investigated the dynamic characteristics of water droplets, their effect on insulator performance and their connection to surface discharges [15], [16], [17], [18], [19], [20], [22], [23], [24], [25].

In [15] and [16], the impact of water droplets on partial discharge and electric field distribution was studied. Another study investigated the interaction between water droplets and electric potential distribution [17]. The study [18], [19] explored the corona discharge effect arising from water droplets on the surface of a polymer insulator.

Discharge occurrences near separate water droplets on different hydrophobic insulator surfaces, employing electric field and energy calculations, were investigated in [20]. In [21], various surface discharge characteristics, including energy, were influenced by factors such as droplet dimensions, shape, spacing, and position [21]. Furthermore, a theoretical model assessing discharge behaviour with water contamination was developed [22].

In [23], joint measurements of leakage current and partial discharges on silicone rubber insulators exposed to salt fog were investigated using pattern recognition. The study revealed that partial discharge sensitivity identifies the shift from corona activity to arcing discharges under dry conditions [23].

In [24], the interaction between water droplets and the external electric field was investigated. These interrelations are evaluated by the surface hydrophobic properties and evidently prevent weak corona discharge [24]. The threshold voltage of partial discharge is a transition corresponding to a change in the oscillation pattern of water droplets. This transition remains unaffected by the conductivity of water droplets on surfaces with greater hydrophobicity [25].

The study findings indicate that water droplets alter the electric field and voltage distribution on the insulator's surface, potentially causing corona discharges and breakdown. This underscores the importance of studying insulator surfaces with water droplets.

With the advent of deep learning techniques and their numerous applications in engineering, previously a convolutional neural network (CNN) was proposed as the backbone data analysis used to classify contaminated insulator surfaces [1]. Specifically, a brute-force model selection method within a limited hyperparameter space enabled the classification of contaminated insulator surfaces. In this study, the specific focus is on ensemble learning techniques, where predictions from multiple deep CNN architectures are combined to obtain a more robust model.

Ensemble learning combines predictions from several base models to achieve a tradeoff between bias and variance, and that may lead to a better performance than a single predictive model [27]. Unlike a single model, which may overfit, a proper combination of predictions from several base models may lead to more robust predictive models [27]. The power of the ensemble model to improve the efficacy of base models makes it a promising tool for HV insulator inspection. In this paper, it was proposed a novel stacked ensemble learning rule that employs several pretrained deep CNN architectures to classify clean overhead insulator surfaces from surfaces covered with water droplets. The main contributions of this paper are as follows:

- In contrast with the usual approach in which an individual pretrained CNN architecture is selected, tuned, and used, it was proposed a novel stacked ensemble learning rule that selects the "best" subset of pretrained architectures for the classification of insulator surface contamination. The results show the advantage of the proposed learning rule compared with the usual approach.
- A new HV insulator surface contamination dataset is built, which includes both laboratory-based as well as artificially generated images to train contaminated insulator surface classifiers. Specifically, for future studies, this dataset can be combined with different insulator datasets to form insulator-agnostic classifiers of surface contamination in the electricity distribution grid.

The rest of the paper is organized as follows. Section II covers advanced techniques used in HV insulator analysis. Section III presents experimental results. This section discusses the data collection procedure, learning, and evaluation of the proposed learning rule. Section IV summarizes our observations, presents some limitations of the present work, and put forward possible future directions that can be explored. Finally, Section V concludes the paper.

II. ADVANCED TECHNIQUES AND METHODOLOGY
A. ADVANCED TECHNIQUES
Conventional methods of power line inspection require engineers to patrol the HV insulators on foot or clime the poles to determine possible faults. Expanding electricity transmission lines to secluded areas makes monitoring with the previously mentioned methods inaccessible and difficult. Therefore, applying advanced machine learning (ML) including deep

learning techniques is an effective strategy for power line analysis, and that appears to be a plausible option for synchronized monitoring applications [28]. Said that implementing ML techniques requires data collection in the first place.

Collecting a large quantity of data while performing a specific domain-related task is challenging. Constructing a satisfactory classifier model based on only a limited quantity of training data is also difficult, if not impossible. To address the data scarcity problem, one of the possible solutions is transfer learning. Transfer learning studies effective ways to train effective predictive models in a target domain, where there is a lack of data, from models trained using a large amount of data from a source domain; for example, adapting a model trained on large image classification datasets to our power line inspection application with a limited number of insulator images. In this regard, a pretrained model requires fine-tuning using the dataset collected from the target domain. In some HV insulator condition analyses, pretrained models have already been deployed. In [29], authors proposed a MobileNet-based model that improves the detection of power line insulator defects. To solve the low detection speed of the YOLOv4 object detection model, a method for detecting defects in a power line insulator based on the improved YOLOv4 algorithm with MobileNet was proposed. The results show that the trained model using 2403 images achieved a detection accuracy of 93.81% with a speed of 53 frames per second compared with the original YOLOv4.

For faulty insulator images with noisy backgrounds, a Cross Stage Partial Dense (CSPD) YOLO model was proposed in [30]. First, a new dataset with 1331 aerial images was collected and built for training. Then, the CSPD network was proposed to extract useful features of the YOLOv3 model based on the Cross Stage Partial Network, YOLOv3, and DenseNet. For better feature extraction and faulty insulator detection, feature fusion, k-mean clustering, and an improved loss function were used. Empirical results showed that the proposed CSPD-YOLO model outperformed the YOLOv3 and YOLOv4 models in terms of average precision, however, falls behind ($\sim$0.011s) in terms of the average fault detection time.

Recently, many faulty insulator detections based on image processing started using different semantic segmentation techniques [31], [32], [33]. Focusing on faulty insulator detection using HV insulator images, in [31], authors used a semantic segmentation method, namely, DeepLabV3, for extracting insulator masks with cluttered background data and cascading it with the target detector YOLOv3. Using 600 insulator images, DeepLabv3 was compared with other popular semantic segmentation techniques such as SegNet, PSPNet, and U-Net. In general, faulty insulator detection with noisy background images is an arduous task. In this regard, an application of the cascaded model with two networks for detection and segmentation is proposed in [32]. First, an improved Faster R-CNN model was used to detect the faults in the image. In the feature extraction step, the

TABLE 1. Deep learning algorithms used in HV insulator condition analysis.

Model	Problem	Dataset size	Validation accuracy	Test accuracy	References
InceptionV3	to detect pin corrosion, pin and cap separation, partial breakage, and the complete shattering of the dielectric shell (broken insulators)	848	0.957	-	[34]
	to classify freezing, wet, and snowing insulator surface conditions	4 000		0.560	[35]
DenseNet121	to detect pin corrosion, pin and cap separation, partial breakage, and the complete shattering of the dielectric shell (broken insulators)	848	0.992	-	[34]
MobileNet	to detect pin corrosion, pin and cap separation, partial breakage, and the complete shattering of the dielectric shell (broken insulators)	848	0.984	-	[34]
	to classify freezing, wet, and snowing insulator surface conditions	4 000	-	0.410	[35]
EfficientNet	to detect missing insulator disks	2 000	0.951	-	[36]
Xception	to detect pin corrosion, pin and cap separation, partial breakage, and the complete shattering of the dielectric shell (broken insulators)	848	0.981	-	[37]
ResNet50	to evaluate silicone rubber material surface erosion	1 810	-	0.998	[37]
	to detect pin corrosion, pin and cap separation, partial breakage, and the complete shattering of the dielectric shell (broken insulators)	848	0.926	-	[34]
	to detect missing insulator disks	2 000	-	0.932	[36]
	to classify wettability conditions of the polymeric insulator surface (form I to VII)	840		0.945	[38]
	to classify freezing, wet, and snowing insulator surface conditions	4 000	-	0.610	[38]

ResNeXt-101 with FPN was used. To address the imbalanced training samples, an Online Hard Example Mining (OHEM) algorithm was also utilized. Furthermore, a U-net was proposed to extract objects from insulator images and combines deep and shallow features for the classification and localization of pixels. This experiment shows the utility of the proposed method to detect faults from ceramic insulator images with a cluttered background. The training results show high precision and recall values of 91.9% and 95.7%, respectively.

In [33], 620 high-resolution images of HV insulators are collected by helicopters. The self-blast glass insulator detection problem is addressed by deep learning techniques and divided into two subproblems: object detection and semantic segmentation. The results show that Faster R- CNN and InceptionResNetv2 pretrained models reached 95.1% and 95.5% in terms of precision and recall, respectively.

Many pretrained models have been used in HV insulator condition monitoring. Detailed information on transfer learning techniques used for HV insulator analysis is presented in Table 1 [34], [35], [36], [37], [38].

B. STACKED ENSEMBLE LEARNING
Stacked ensemble learning (also known as a stacked generalization) is commonly viewed as a method for combining the outcomes of N base models (also known as level-0 generalizers) using another model (level-1 generalizer) that is trained based on the outputs of the base models along with the desired outcomes [39], [40] (see Fig. 1). Stacked generalization is a general and diverse learning strategy that includes various other common techniques. For instance, consider the common approach of the ''winner-takes-all'' strategy. In this strategy, out of several generalizers (classifiers or regressors), a single generalizer with the best performance, e.g., the highest accuracy in classification, on a validation set (or using cross-validation) is selected for performing prediction

on unseen data. This is in itself a stacked generalization that in Wolpert's words [39], has ''an extraordinary dumb level-1 generalizer'' that selects the level-0 generalizer with the lowest estimated error. The level-1 generalizers used in stacked ensemble learning are usually more intelligent than this.

In this work, it was proposed a stacked ensemble learning (Fig. 1) based on the following two assumptions: 1) due to the limited size of the insulator dataset, a number of pretrained deep neural networks (DNNs) such as InceptionV3 [41], DenseNet121 [42], MobileNet [43], EfficientNetB2 [44], [45], Xception [46], and ResNet50 [47] are proposed as base models for our level-0 generalizers.

To be exact, these models were fine-tuned, where the frozen convolutional base serves as a feature extractor and is followed by a dense layer trained using an insulator dataset for classifying the insulator surface. This is because each of these DNNs has a strong history in image classification applications, and 2) as the level-1 generalizer, we use the majority vote among a selected subset of decisions made by level-0 generalizers. The level-1 generalizer learns (identifies) the best subsets of level-0 generalizers in terms of achieving the highest accuracy using a majority vote. The rationale behind this approach is that there are no guarantees that using all level-0 classifiers as the input to the majority vote is necessarily the most prudent way to go about final decision-making.

The question is whether we can learn to select the best subset of level-0 generalizers to maximize generalization performance. Learning the ''best'' subset of level-0 generalizers is achieved by training a level-1 generalizer. The level-1 generalizer is learned by applying an exhaustive search for model subset selection.

Specifically, the computational complexity of testing all six pretrained models requires evaluating $2^6-1 = 63$ different model subsets. However, to avoid ties in decision-making
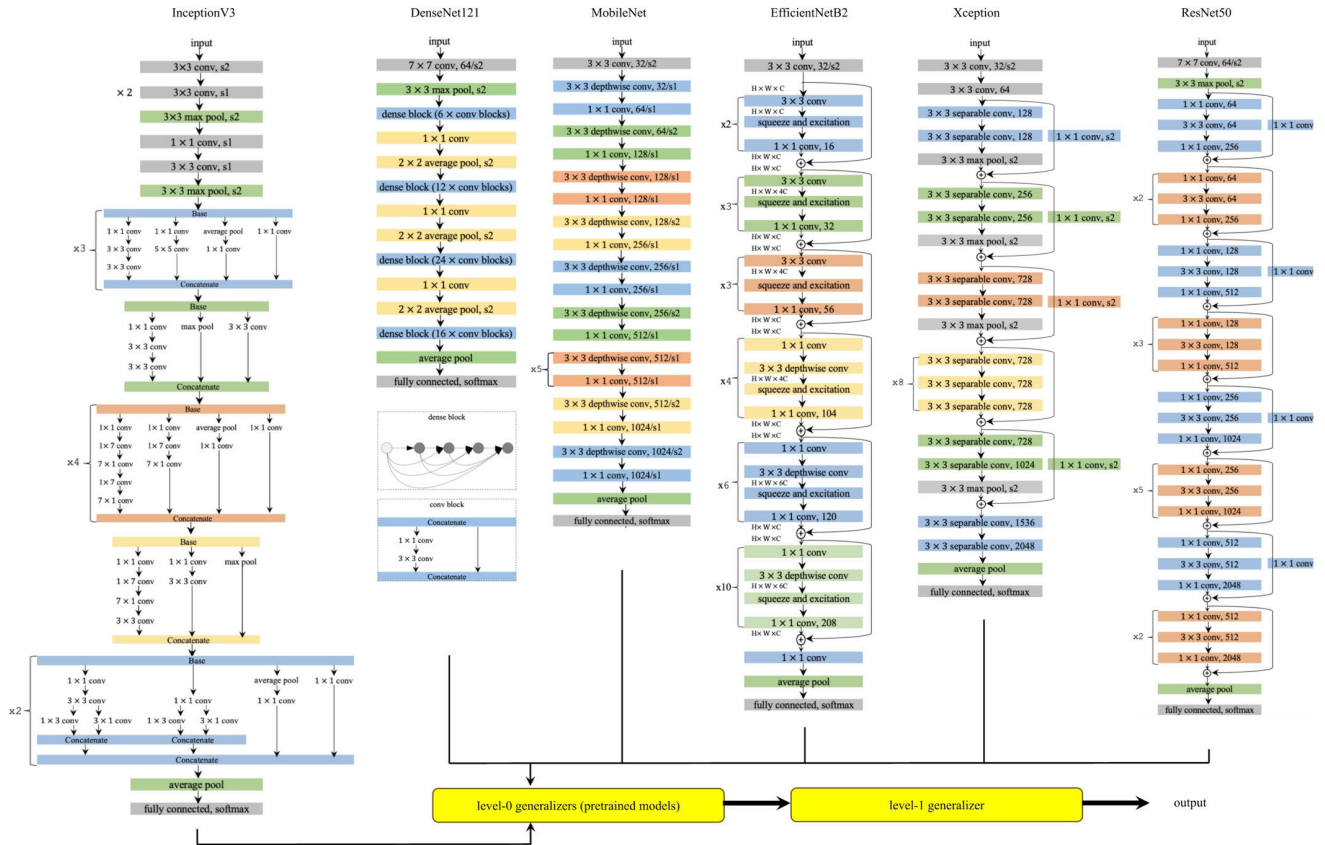
FIGURE 1. Schematic representation of stacking-based ensemble learning (stacked generalization).

by the majority vote, subsets with an odd number of level-0 generalizers are only searched through. As, if majority voting takes an even number of models (2, 4, or 6) as input, it may lead to a tie problem with similar votes for each class. Therefore, only an odd number of models are used to address the tie-breaking problem. Consequently, in addition to the six individual models, it was also considered 26 subsets containing 3 or 5 level-0 generalizers.

III. EXPERIMENTAL STUDY
A. TEST OBJECTS, MAIN GOALS, AND DATA COLLECTION
According to the International Electrotechnical Commission (IEC) technical specifications [9], [10], there exist three main aspects affecting insulator contamination. The contamination itself, humidification, and insulator layout characteristics. In this study, the first aspect is particularly focused, and two insulator surface conditions are considered: normal and polluted high-voltage insulators and it was employed stacked ensemble learning based on pretrained deep CNNs for analysis. The main purpose of this research work is to build a model for classifying a clean insulator surface from those sprayed with water droplets for porcelain (ceramic) and polymer

(rubber-post) insulator surfaces using the stacked ensemble learning rule. Water droplet contamination was used as it is quite common and frequently takes place over insulators all over the countries. The model developed in this study can be then extended and examined over other contamination categories such as cement and metal particles, salty water, corrosions, dust, etc.

In image processing tasks, the classification of insulator types such as porcelain (ceramic) and polymer (rubber-post) does not bear significance. In contrast, in cases quantifying electrical properties, the insulating material's composition may indeed hold importance. In this paper, since the proposed method involves the application of image processing, the specific type of material holds no significant relevance.

Several studies on tools made of different materials, but subjected to the same operating conditions, were grouped into a singular category, showing significant findings [48], [49], [50], [51]. In [48], five types of solar panels were used to collect data on different types of contamination. Similarly, a stacked ensemble learning technique was employed to explore traffic sign recognition [49], malware detection [50], and sand-dust storm forecasting [50]. These

examples allowed us to streamline this method while still capturing the impact of different insulator materials under the same weather conditions.

A proposed unified approach that considers different materials together is applicable to different conditions, ensuring practicality in real-world cases where the insulator type may not always be known.

Unstable weather conditions cause complications for power companies in the formulation of standards and insulator condition monitoring systems. In this regard, there are several available regulations that provide distinct technical specifications for the selection, dimensioning, and cleaning of overhead line insulators: the IEC/TS 60815 [9], the CIGRE technical brochures (Working Group C4.303) [8], the Electric Power Research Institute standard (EPRI) [52], the Swedish Transmission Research Institute guide (STRI) [53], the Institute of Electrical and Electronics Engineers standard 957 (IEEE) [6], the United States Patent [5], and the Guidance Document 34.51.503-93 (GD) [54].

However, there is no specific established and open-access dataset available for insulator condition inspection. Since defected high-voltage insulators are difficult to access, large-scale dataset construction may become an arduous task for many transmission line monitoring utilities. Therefore, a new insulator dataset (see Fig. 2) composed of 239 images of ceramic and rubber-post insulators was collected (see [1] for details) in HV and Power System Laboratory. The findings of this research are relevant to both rubber-post and ceramic insulators and can be applied to both materials. Also, the type of insulator material is not distinguished during the classification. The dataset contains insulator surfaces for two different conditions clean and artificially contaminated with water drops. The data collection procedure has two stages: the artificial contamination stage and taking pictures. Insulator surfaces are sprayed with tap water to reach an artificial pollution layer that simulates rainy weather. Afterwards, the insulator images are collected from different shooting angles under usual inhomogeneous illumination and background conditions. The insulator images are collected in the Power System Laboratory at an average room temperature of ~21°C and humidity of ~45%.

For training classifiers, the dataset was split into three sets (70% training, 15% test and 15% validation). Data augmentation techniques such as rotation (100), rescaling (1/255), width and height shift range (10%), fill mode (nearest), shear (0.1 rad) and zoom mode (10%) were applied to training data to create 761 additional images [1]. Some samples of augmented insulator images are shown in Fig. 4.

To collect the images, the DJI Mavic 2 Zoom was used as a digital imaging device, and its flight features are detailed in Table 2.

All experiments were conducted on a Windows 10 Pro with an Intel (R) Core (TM) i9-9900 CPU, 3.10 GHz, and 8 GB of RAM. The entire workflow was implemented in TensorFlow 2.10.

(a) Clean   (b) Contaminated with water droplets
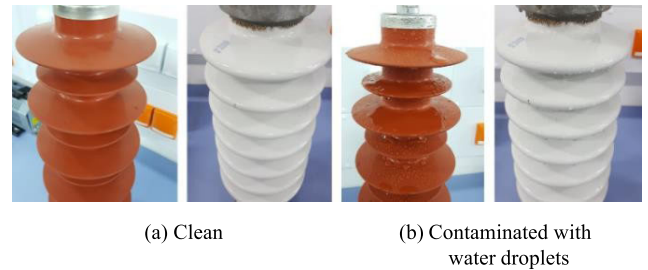
FIGURE 2. High-voltage insulator surfaces with (a) a clean surface and (b) water droplets [1].

B. LEARNING THE STACKED GENERALIZER

Each pretrained model (see Table 3) is trained separately with a fixed convolutional base followed by a dense layer that is trained based on the given training data to classify surface conditions. In this regard, the six aforementioned pretrained architectures (see Section II) were trained and used as level-0 generalizers. For each architecture, the weights of the dense layer at the epoch that led to the highest accuracy on the validation set were used. As mentioned before, here training the level-1 generalizer (i.e., the majority vote on a subset of level-0 generalizers) merely includes finding the "best" subset with an odd number of level-0 generalizers. This is achieved by finding the subset of level-0 generalizers whose majority vote leads to the highest accuracy on the validation set. As a result, the validation set is used for two purposes: 1) tuning the epoch for individual level-0 generalizers; and 2) training the level-1 generalizer. The latter would make more sense when it is compared this training stage (training level-1 generalizer) to the training of the aforementioned "extraordinary dumb level-1 generalizer" (i.e., winner-takes-all) that is performed on the validation set per se (see Table 3).

To mitigate redundancy and optimize space utilization, a model identifier was assigned to each level-0 generalizer subset, as follows: MobileNet denoted as 'a', EfficientNetB2 as 'b', ResNet50 as 'c', Xception as 'd', InceptionV3 as 'e', and DenseNet121 as 'f'.

Table 3 shows the estimated accuracy for each individual level-0 generalizer as well as the 26 subsets of 3 or 5 level-0 generalizers. These results are visualized in Fig. 3 and compared against the highest accuracy achieved by individual pretrained models—this accuracy is 68.6%, which is achieved by ResNet50 and is identified by the dashed horizontal line in Fig. 3. As one of the objectives of our analysis is to examine the performance of the proposed stacked ensemble learning scheme with respect to the best individual model, the 68.6% accuracy obtained on the validation set using ResNet50 is referred to as the "baseline" accuracy. From Fig. 3 it is observed that 7 combinations of models achieved an accuracy that is higher than the baseline. Table 3 shows these combinations and the number of parameters involved in their structures.

The results presented in Table 3 show that the ensemble classifier constructed by EfficientNetB2, ResNet50, and
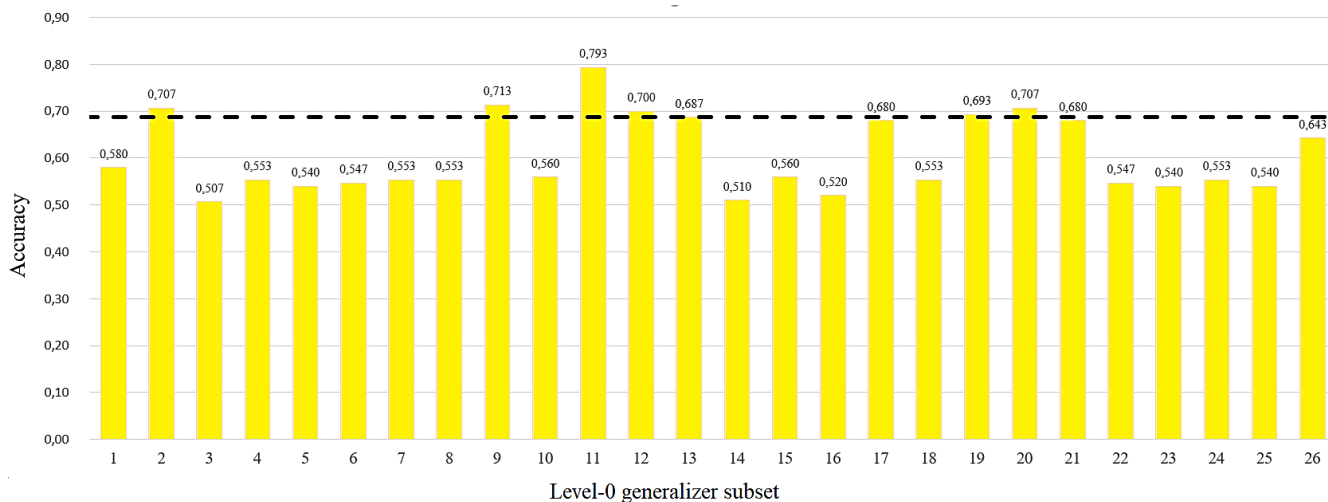
FIGURE 3. The performance of level-0 generalizer subsets on the validation set. Each subset is identified by an index that is assigned to the subset in Table 3. The horizontal dashed line shows the baseline; that is, the highest accuracy achieved by any of the individual level-0 generalizers on the validation set.

Xception (identified by ''b-c-d'' in the table) achieved the highest accuracy on the validation set, which is 79.3%. If only the performance metric is taken into account, one should naturally select the ''b-c-d'' classifier as the ''best'' model. However, it can be noted from Table 4 that this model has the second highest complexity in terms of the number of parameters—it includes 57.8 M parameters. At the same time, note that all models in Table 4 exhibited better performance than the baseline. Therefore, it would be valuable to also consider the complexity of these models in addition to the performance metric to determine the ''best'' model.

From Tables 3 and 4, it is observed that the second best model in terms of estimated accuracy on the validation set (i.e., ''a-d-f'') has, interestingly, the lowest number of parameters in Table 4 (i.e., 35.3 M). As a result of these observations, a definite selection is not made between ''b-c-d'' and ''a-d-f''; that is to say, the level-1 generalizer utilizes ''a-d-f'' based on its considerably lower computational complexity, whereas uses ''b-c-d'' based on its high performance. Said that, in the next stage, both architectures will be evaluated on the test set to examine their performance and make recommendations.

C. EVALUATION
As the result of the model subset selection rule that is indeed part of the level-1 generalizer training, both ensemble classifiers identified by ''b-c-d'' and ''a-d-f'' in Table 4, are evaluated on the test set. The results show that ''b-c-d'' and ''a- d-f'' achieved an accuracy of 73.3% and 64.7% on the test set, respectively. For the sake of comparison, ResNet50 is also evaluated, which is the level-0 generalizer that achieved the highest accuracy on the validation set. The results show that ResNet50 achieved an accuracy of 57.8%, which is considerably lower than the accuracy of the ''b-c-d'' and ''a-d-f'' ensemble classifiers on the test set. This observation confirms

TABLE 2. DJI Mavic 2 zoom flight features.

Resolution	12 MP
Aperture	f/2.8
Focal length	24-48 mm
Shutter speed	8–1/8000 s
Sensor size	1/2.3 inch

the efficacy of our proposed stacked ensemble learning strategy based on a combination of well-known pretrained CNN architectures. As a result of the proposed stacked ensemble learning rule, our recommendation is to utilize the majority vote with EfficientNetB2-ResNet50-Xception when maximum performance is desired; however, for embedded devices with limited memory/computing power, using the majority vote with MobileNet-DenseNet121-Xception would provide a reasonable tradeoff between complexity and performance. MobileNet-DenseNet121-Xception has ∼39% fewer parameters compared with EfficientNetB2-ResNet50-Xception.

IV. DISCUSSION
In this study, it was proposed a novel stacked ensemble learning rule based on six pretrained CNNs, which are used as level-0 generalizers in the stacked structure, to classify high-voltage insulator surface conditions. The choice of level-0 generalizers is MobileNet, EfficientNetB2, ResNet50, Xception, InceptionV3, and DenseNet121. The rationale for choosing these architectures is that each of them has a strong track record in image classification applications. For the level-1 generalizer, we use the majority vote among a selected subset of decisions made by level-0 generalizers. The rationale behind model subset selection is that there are no guarantees that including all level-0 generalizers, as the input to the majority vote, will necessarily lead to the highest classification accuracy.
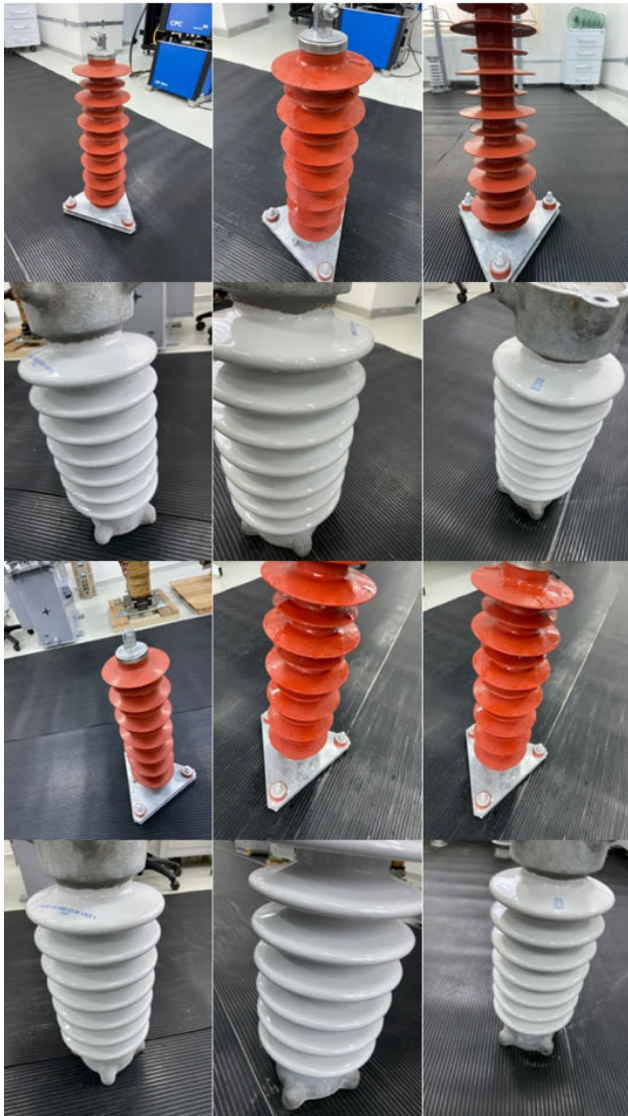
FIGURE 4. Augmented insulator images samples.

TABLE 3. Accuracies of level-0 Generalizers and their subsets on the validation set. Each pretrained model is identified by a letter, and their combination is identified by a combination of corresponding letters.

		Model identifier: model name	Validation Accuracy
Level-0 generalizers		a: MobileNet	0.540
		b: EfficientNetB2	0.500
		c: ResNet50	0.686
		d: Xception	0.546
		e: InceptionV3	0.560
		f: DenseNet121	0.546
Level-0 generalizer subsets	1	a-b-c	0.580
	2	a-b-d	0.706
	3	a-b-e	0.506
	4	a-b-f	0.553
	5	a-c-d	0.540
	6	a-c-e	0.546
	7	a-c-f	0.553
	8	a-d-e	0.553
	9	a-d-f	0.713
	10	a-e-f	0.560
	11	**b-c-d**	**0.793**
	12	b-c-e	0.700
	13	b-c-f	0.686
	14	b-d-e	0.510
	15	b-d-f	0.560
	16	b-e-f	0.520
	17	c-d-e	0.680
	18	c-d-f	0.553
	19	c-e-f	0.693
	20	d-e-f	0.706
	21	a-b-c-d-e	0.680
	22	a-b-c-d-f	0.546
	23	a-b-c-e-f	0.540
	24	a-b-d-e-f	0.553
	25	a-c-d-e-f	0.540
	26	b-c-d-e-f	0.643

To train the level-1 generalizer or, equivalently, to determine the model subset (with the majority vote) that leads to the highest accuracy on the validation set, it was considered both the estimate of the performance metric on the validation set and the complexity of the model in terms of a number of parameters. The complexity factor plays an important role when it considers the potential implementation of the developed classifier over resource-limited embedded devices. This strategy pointed to the use of a majority vote with two combinations of pretrained architectures: 1) EfficientNetB2-ResNet50-Xception; and 2) MobileNet-DenseNet121-Xception. Our recommendation is to utilize the former combination when maximum performance is desired while using the latter when computational efficiency is required at the expense of a reduction in performance.

One limitation of our work is the number of images used in the original training set before data augmentation. We acknowledge that our sample size is smaller than the typical sample size used for training deep neural networks. However, it is quite impressive that even with this small number of images used in our stacked ensemble deep learning approach, we can obtain 73.3% on the test set. The result of this study paves the way to examine our proposed approach using larger datasets. That being said, we have already initiated the process of collecting images from a variety of insulators under a number of more environmental conditions. However, this process is laborious and takes time. As a result, we leave investigating the performance of the proposed approach here in those settings for future studies. Another related limitation is that here only two classes of insulator surfaces are considered; that is, clean and contaminated, and the contaminated condition only considered raindrops. However, in practice, contamination could be in many other forms such as dust, snow, and cement, to just name a few. As a result, the robustness of the constructed models should be examined here on other forms of contamination. To this end, a comprehensive dataset of different contamination types over a range of different insulators first needs to be collected. Once the data is collected, our selected models here

	Level-0 generalizer subsets	Level-0 generalizers	Number of parameters	Total number of parameters
2	a-b-d	MobileNet	4.3 M	36.5 M
		EfficientNetB2	9.2 M	
		Xception	23 M	
9	a-d-f	MobileNet	4.3 M	35.3 M
		Xception	23 M	
		DenseNet121	8 M	
11	b-c-d	EfficientNetB2	9.2 M	57.8 M
		ResNet50	25.6 M	
		Xception	23 M	
12	b-c-e	EfficientNetB2	9.2 M	58.7 M
		ResNet50	25.6 M	
		InceptionV3	23.9 M	
13	b-c-f	EfficientNetB2	9.2 M	42.8 M
		ResNet50	25.6 M	
		DenseNet121	8 M	
19	c-e-f	ResNet50	25.6 M	57.5 M
		InceptionV3	23.9 M	
		DenseNet121	8 M	
20	d-e-f	Xception	23 M	54.9 M
		InceptionV3	23.9 M	
		DenseNet121	8 M	

may be fine-tuned and their predictive performance checked. Should our selected models fail in predictive performance, the proposed stacked ensemble classifier will be retrained, which may lead to a new combination of the pretrained architectures.

Another limitation in the present work, which also extends to some of our previous studies [1], [55], [56], is the utility of artificial contamination. The high-voltage laboratory condition was utilized to emulate the insulators' contamination (in this study specifically raindrops), and all data in this study were collected in a laboratory environment. Even though emulating raindrops in a laboratory environment is quite straightforward, the robustness of developed models in real environmental conditions should be examined. Nonetheless, artificial pollution emulation in the laboratory is faster and more feasible and it can help identify the insulator's capability to deal with a predetermined intensity of moistened pollution. The field pollution examination and data collection will be able to completely satisfy and meet real operational conditions as it reveals both the degree of the insulator surface pollution severity for a specific setting and the capability of the corresponding insulator, under voltage stress, to resist the deposition of pollution when moistened with the rain. Undoubtedly, the results of the examination carried out in a relevant outdoor setting and in an indoor chamber with artificial contamination will give the most accurate predictions for monitoring the condition of the insulator under different weather conditions.

V. CONCLUSION
The high-voltage insulator's prognosis techniques were widely discussed and different solutions to evaluate the insulator surface condition were highlighted. Two ceramic and rubber-post insulators in normal and raindrop contamination conditions were studied and examined. Our empirical results revealed that for insulator surface condition classification, the proposed stacked ensemble learning rule based on pretrained deep CNN architectures can outperform any of the individual architectures used as part of its structure. This is in sharp contrast with the usual "winner-takes-all" model selection strategy in which a practitioner selects, tunes, and uses a single pretrained architecture. Indeed, using intelligent techniques in remote monitoring of high-voltage insulator conditions requires an accurate classifier model. Using a stacked ensemble learning model for the first time in the high-voltage field here, this study can serve as a catalyst for a rich set of research problems to implement various ensemble learning algorithms successfully and accurately in overhead line inspection.

REFERENCES
[1] A. Serikbay, M. Bagheri, and A. Zollanvari, "High voltage insulators condition analysis using convolutional neural network," in Proc. IEEE Int. Conf. Environ. Electr. Eng., IEEE Ind. Commercial Power Syst. Eur. (EEEIC/I&CPS Eur.), Sep. 2021, pp. 1–5, doi: 10.1109/EEEIC/ICPSEurope51590.2021.9584624.

[2] S.-H. Kim, E. A. Cherney, and R. Hackam, "Hydrophobic behavior of insulators coated with RTV silicone rubber," IEEE Trans. Electr. Insul., vol. 27, no. 3, pp. 610–622, Jun. 1992, doi: 10.1109/14.142726.

[3] M. Taghvaei, M. Sedighizadeh, N. NayebPashaee, and A. S. Fini, "Reliability assessment of RTV and nano-RTV-coated insulators concerning contamination severity," Electr. Power Syst. Res., vol. 191, Feb. 2021, Art. no. 106892, doi: 10.1016/j.epsr.2020.106892.

[4] H. de Santos and M. Á. Sanz-Bobi, "Research on the pollution performance and degradation of superhydrophobic nano-coatings for toughened glass insulators," Electr. Power Syst. Res., vol. 191, Feb. 2021, Art. no. 106863, doi: 10.1016/j.epsr.2020.106863.

[5] M. Al-Hamouz and L. Sulyman, "Contamination level estimation method for high voltage insulators," U.S. Patent 9 384 560 B2, 2016, p. 15, vol. 2, no. 12, doi: 10.3390/en15207656.

[6] IEEE Guide for Cleaning Insulators, IEEE Standard 957, IEEE Power Engineering Society, 2005, pp. 1–64.

[7] L. An, X. Jiang, and Z. Han, "Measurements of equivalent salt deposit density (ESDD) on a suspension insulator," IEEE Trans. Dielectr. Electr. Insul., vol. 9, no. 4, pp. 562–568, Aug. 2002, doi: 10.1109/TDEI.2002.1024434.

[8] Outdoor Insulation in Polluted Conditions: Guidelines for Selection and Dimensioning. Part 1: General Principles and the AC Case, CIGRE, Paris, France, Jun. 2008, p. 58.

[9] Selection and Dimensioning of High-Voltage Insulators Intended for Use in Polluted Conditions—Part 1: Definitions, Information and General Principles, Standard IEC TS 60815-1, International Electrotechnical Commission, 2018, pp. 1–2.

[10] Artificial Pollution Tests on High-Voltage Ceramic and Glass Insulators to be Used on A.C. Systems, Standard IEC 60507, 2013.

[11] L. Maraaba, Z. Al-Hamouz, and H. Al-Duwaish, "Prediction of the levels of contamination of HV insulators using image linear algebraic features and neural networks," Arabian J. Sci. Eng., vol. 40, no. 9, pp. 2609–2617, Sep. 2015, doi: 10.1007/s13369-015-1704-z.

[12] D. Zhang, H. Xu, J. Liu, C. Yang, X. Huang, Z. Zhang, and X. Jiang, "Research on the non-contact pollution monitoring method of composite insulator based on space electric field," Energies, vol. 14, no. 8, pp. 1–15, 2021, doi: 10.3390/en14082116.

[13] S. Sanyal, T. Kim, J.-B. Koo, J.-A. Son, I.-H. Choi, and J. Yi, "Probabilistic analysis of the failure of high-voltage insulators based on compositional analysis," Electr. Power Syst. Res., vol. 195, Jun. 2021, Art. no. 107184, doi: 10.1016/j.epsr.2021.107184.

[14] Y. Huang, X. Jiang, and M. S. Virk, "Ice accretion study of FXBW4-220 transmission line composite insulators and anti-icing geometry optimization," *Electr. Power Syst. Res.*, vol. 194, May 2021, Art. no. 107089, doi: 10.1016/j.epsr.2021.107089.

[15] H. Gao, Z. Jia, Y. Mao, Z. Guan, and L. Wang, "Effect of hydrophobicity on electric field distribution and discharges along various wetted hydrophobic surfaces," *IEEE Trans. Dielectr. Electr. Insul.*, vol. 15, no. 2, pp. 435–443, Apr. 2008, doi: 10.1109/TDEI.2008.4483462.

[16] C. Zixia, L. Xidong, Z. Yuanxiang, W. Shaowu, and G. Zhicheng, "Study of water droplet discharge by electric field computation and high-speed video," in *Proc. IEEE 7th Int. Conf. Properties Appl. Dielectr. Mater.*, Nagoya, Japan, vol. 2, Jun. 2003, pp. 820–823, doi: 10.1109/ICPADM.2003.1218545.

[17] Waluyo, P. Pakpahan, and Suwarno, "Influences of water droplet size and contact angle on the electric field and potential distributions on an insulator surface," in *Proc. IEEE 8th Int. Conf. Properties Appl. Dielectr. Mater.*, Bali, Indonesia, Jun. 2006, pp. 889–892, doi: 10.1109/ICPADM.2006.284320.

[18] Y. Zhu, M. Otsubo, C. Honda, and S. Tanaka, "Corona discharge from water droplet on electrically stressed polymer surface," *Jpn. J. Appl. Phys.*, vol. 45, no. 1A, pp. 234–238, Jan. 2006, doi: 10.1143/JJAP.45.234.

[19] K. Katada, Y. Takada, M. Takano, T. Nakanishi, Y. Hayashi, and R. Matsuoka, "Corona discharge characteristics of water droplets on hydrophobic polymer insulator surface," in *Proc. IEEE 6th Int. Conf. Properties Appl. Dielectr. Mater.*, vol. 2, Jun. 2000, pp. 781–784, doi: 10.1109/ICPADM.2000.876346.

[20] H. El-Kishky and R. S. Gorur, "Electric field computation on an insulating surface with discrete water droplets," *IEEE Trans. Dielectr. Electr. Insul.*, vol. 3, no. 3, pp. 450–456, Jun. 1996.

[21] H. El-Kishky and R. S. Gorur, "Electric field and energy computation on wet insulating surfaces," *IEEE Trans. Dielectr. Electr. Insul.*, vol. 3, no. 4, pp. 587–593, Aug. 1996.

[22] L. Bo and R. S. Gorur, "Modeling flashover of AC outdoor insulators under contaminated conditions with dry band formation and arcing," *IEEE Trans. Dielectr. Electr. Insul.*, vol. 19, no. 3, pp. 1037–1043, Jun. 2012.

[23] I. J. S. Lopes, S. H. Jayaram, and E. A. Cherney, "A method for detecting the transition from corona from water droplets to dry-band arcing on silicone rubber insulators," *IEEE Trans. Dielectr. Electr. Insul.*, vol. 9, no. 6, pp. 964–971, Dec. 2002.

[24] H. Gao, Z. Jia, Y. Mao, Z. Guan, and L. Wang, "Effect of hydrophobicity on electric field distribution and discharges along various wetted hydrophobic surfaces," *IEEE Trans. Dielectr. Electr. Insul.*, vol. 15, no. 2, pp. 435–443, Apr. 2008.

[25] M. H. Nazemi and V. Hinrichsen, "Experimental investigations on water droplet oscillation and partial discharge inception voltage on polymeric insulating surfaces under the influence of AC electric field stress," *IEEE Trans. Dielectr. Electr. Insul.*, vol. 20, no. 2, pp. 443–453, Apr. 2013.

[26] J. W. Busby, K. Baker, M. D. Bazilian, A. Q. Gilbert, E. Grubert, V. Rai, J. D. Rhodes, S. Shidore, C. A. Smith, and M. E. Webber, "Cascading risks: Understanding the 2021 winter blackout in Texas," *Energy Res. Social Sci.*, vol. 77, Jul. 2021, Art. no. 102106, doi: 10.1016/j.erss.2021.102106.

[27] T. Aboneh, A. Rorissa, and R. Srinivasagan, "Stacking-based ensemble learning method for multi-spectral image classification," *Technologies*, vol. 10, no. 17, pp. 1–18, 2022, doi: 10.3390/technologies10010017.

[28] P. S. Prasad and B. P. Rao, "Review on machine vision based insulator inspection systems for power distribution system," *J. Eng. Sci. Technol. Rev.*, vol. 9, no. 5, pp. 135–141, Oct. 2016, doi: 10.25103/jestr.095.21.

[29] Z. Ling, D. Zhang, R. C. Qiu, Z. Jin, Y. Zhang, X. He, and H. Liu, "An accurate and real-time method of self-blast glass insulator location based on faster R-CNN and U-Net with aerial images," *CSEE J. Power Energy Syst.*, vol. 5, no. 4, pp. 474–482, Dec. 2019, doi: 10.17775/CSEE-JPES.2019.00460.

[30] Z. Qiu, X. Zhu, C. Liao, D. Shi, and W. Qu, "Detection of transmission line insulator defects based on an improved lightweight YOLOv4 model," *Appl. Sci.*, vol. 12, no. 3, p. 1207, Jan. 2022, doi: 10.3390/app12031207.

[31] C. Liu, Y. Wu, J. Liu, Z. Sun, and H. Xu, "Insulator faults detection in aerial images from high-voltage transmission lines based on deep learning model," *Appl. Sci.*, vol. 11, no. 10, p. 4647, May 2021, doi: 10.3390/app11104647.

[32] S. Wang, Z. Zhou, and W. Zhao, "Semantic segmentation and defect detection of aerial insulators of transmission lines," *J. Phys., Conf. Ser.*, vol. 2185, no. 1, Jan. 2022, Art. no. 012086, doi: 10.1088/1742-6596/2185/1/012086.

[33] X. Li, H. Su, and G. Liu, "Insulator defect recognition based on global detection and local segmentation," *IEEE Access*, vol. 8, pp. 59934–59946, 2020, doi: 10.1109/ACCESS.2020.2982288.

[34] S. Panigrahy, S. Karmakar, and R. Sahoo, "Transfer learning based condition assessment of high voltage insulator: A comparative analysis," in *Proc. IEEE 5th Int. Conf. Condition Assessment Techn. Electr. Syst. (CATCON)*, Kozhikode, India, Dec. 2021, pp. 145–150, doi: 10.1109/CAT-CON52335.2021.9670517.

[35] D. Pernebayeva, A. Irmanova, D. Sadykova, M. Bagheri, and A. James, "High voltage outdoor insulator surface condition evaluation using aerial insulator images," *High Voltage*, vol. 4, no. 3, pp. 178–185, Sep. 2019, doi: 10.1049/hve.2019.0079.

[36] J. Wang, J. Tang, J. Wei, Y. Wei, H. Wang, and M. Qin, "Image classification of missing insulators based on EfficientNet," in *Proc. 5th Int. Conf. Energy, Electr. Power Eng. (CEEPE)*, Chongqing, China, Apr. 2022, pp. 17–21, doi: 10.1109/CEEPE55110.2022.9783390.

[37] Y. E. Haj, A. H. El-Hag, and R. A. Ghunem, "Application of deep-learning via transfer learning to evaluate silicone rubber material surface erosion," *IEEE Trans. Dielectr. Electr. Insul.*, vol. 28, no. 4, pp. 1465–1467, Aug. 2021, doi: 10.1109/TDEI.2021.009617.

[38] S. Chatterjee, S. S. Roy, K. Samanta, and S. Modak, "Sensing wettability condition of insulation surface employing convolutional neural network," *IEEE Sensors Lett.*, vol. 4, no. 7, pp. 1–4, Jul. 2020, doi: 10.1109/LSENS.2020.3002991.

[39] D. H. Wolpert, "Stacked generalization," *Neural Netw.*, vol. 5, no. 2, pp. 241–259, 1992.

[40] A. Mohammed and R. Kora, "A comprehensive review on ensemble deep learning: Opportunities and challenges," *J. King Saud Univ.-Comput. Inf. Sci.*, vol. 35, no. 2, pp. 757–774, Feb. 2023, doi: 10.1016/j.jksuci.2023.01.014.

[41] C. Szegedy, V. Vanhoucke, S. Ioffe, J. Shlens, and Z. Wojna, "Rethinking the inception architecture for computer vision," in *Proc. IEEE Conf. Comput. Vis. Pattern Recognit. (CVPR)*, Jun. 2016, pp. 2818–2826, doi: 10.1109/CVPR.2016.308.

[42] G. Huang, Z. Liu, L. Van Der Maaten, and K. Q. Weinberger, "Densely connected convolutional networks," in *Proc. IEEE Conf. Comput. Vis. Pattern Recognit. (CVPR)*, Jul. 2017, pp. 2261–2269, doi: 10.1109/CVPR.2017.243.

[43] A. G. Howard, M. Zhu, B. Chen, D. Kalenichenko, W. Wang, T. Weyand, M. Andreetto, and H. Adam, "MobileNets: Efficient convolutional neural networks for mobile vision applications," 2017, *arXiv:1704.04861*, doi: 10.48550/arXiv.1704.04861.

[44] M. Tan and Q. V. Le, "EfficientNet: Rethinking model scaling for convolutional neural networks," in *Proc. 36th Int. Conf. Mach. Learn. (ICML)*, Jun. 2019, pp. 10691–10700, doi: 10.48550/arXiv.1905.11946.

[45] M. Tan and Q. V. Le, "EfficientNetV2: Smaller models and faster training," in *Proc. Int. Conf. Mach. Learn.*, 2021, pp. 10096–10106, doi: 10.48550/arXiv.2104.00298.

[46] F. Chollet, "Xception: Deep learning with depthwise separable convolutions," in *Proc. 30th IEEE Conf. Comput. Vis. Pattern Recognit. (CVPR)*, Jul. 2017, pp. 1800–1807, doi: 10.48550/arXiv.1610.02357.

[47] K. He, X. Zhang, S. Ren, and J. Sun, "Deep residual learning for image recognition," in *Proc. IEEE Comput. Soc. Conf. Comput. Vis. Pattern Recognit.*, Jun. 2016, pp. 770–778, doi: 10.48550/arXiv.1512.03385.

[48] P. W. Khan, Y. C. Byun, and O.-R. Jeong, "A stacking ensemble classifier-based machine learning model for classifying pollution sources on photovoltaic panels," *Sci. Rep.*, vol. 13, no. 1, pp. 1–13, Jun. 2023, doi: 10.1038/s41598-023-35476-y.

[49] G. Yildiz, A. Ulu, B. Dızdaroğlu, and D. Yildiz, "Hybrid image improving and CNN (HIICNN) stacking ensemble method for traffic sign recognition," *IEEE Access*, vol. 11, pp. 69536–69552, 2023, doi: 10.1109/ACCESS.2023.3292955.

[50] M. N. Al-Andoli, K. S. Sim, S. C. Tan, P. Y. Goh, and C. P. Lim, "An ensemble-based parallel deep learning classifier with PSO-BP optimization for malware detection," *IEEE Access*, vol. 11, pp. 76330–76346, 2023, doi: 10.1109/ACCESS.2023.3296789.

[51] Q.-D.-E.-J. Ren, N. Li, and W. Zhang, "Research on sand-dust storm forecasting based on deep neural network with stacking ensemble learning," *IEEE Access*, vol. 10, pp. 111855–111863, 2022, doi: 10.1109/ACCESS.2022.3216309.

[52] A. Phillips and T. Shaw, "Field guide: Visual inspection of polymer insulators," Electr. Power Res. Inst. (EPRI), Tech. Rep. 3002005627, 2006, vol. 3, no. 3.

[53] *Hydrophobicity Classification Guide*, Swedish Transmiss. Res. Inst., Ludvika, Sweden, STRI Guide 1, 2005, p. 9.

[54] *Guidelines for Operation of Insulation in Regions With Atmospheric Pollution*, Guidance Document 34.51.503-93 (GD), 1996.

[55] A. Serikbay, M. Bagheri, A. Zollanvari, and B. T. Phung, "Accurate surface condition classification of high voltage insulators based on deep convolutional neural networks," *IEEE Trans. Dielectr. Electr. Insul.*, vol. 28, no. 6, pp. 2126–2133, Dec. 2021, doi: 10.1109/TDEI.2021.009648.

[56] A. Serikbay, M. Bagheri, A. Zollanvari, and A. A. Saukhimov, "CNN-based classification of contaminated high voltage insulator surface," in *Proc. IEEE Int. Conf. Environ. Electr. Eng., IEEE Ind. Commercial Power Syst. Eur. (EEEIC/I&CPS Europe)*, Jun. 2022, pp. 1–5, doi: 10.1109/EEEIC/ICPSEurope54979.2022.9854762.

MEHDI BAGHERI (Senior Member, IEEE) received the Ph.D. degree in electrical power engineering and energy systems from The University of New South Wales (UNSW), Sydney, Australia, in 2014. He was with the Electric Machinery, Motor Drive, and Power Electronics Laboratories, Electrical Engineering Department, National University of Singapore (NUS). He was closely worked with Rolls-Royce Pte. Ltd., on a joint project. Since 2016, he has been with Nazarbayev University, where he is currently an Associate Professor with the Department of Electrical and Computer Engineering. He is actively involved in the advanced testing of industrial projects, and provides technical support to multinational companies, specializing in power product manufacturing, strategic relationships between industry and academia, energy management, smart monitoring of power equipment, and analysis and development of sustainable energy systems. His research interests include high voltage engineering, wireless power transfer, condition monitoring and assessment, diagnosis of power equipment in the field, space, and marine applications, electrical rotating machines, electrical insulation, power quality, and smart energy systems.

He is a member of IEEE PES, IES, and DEIS. In recognition of his contributions to engineering, he received the Scopus Award, in 2022. He is the Head of the Smart Energy Systems Laboratory and has served as a member for the National Research Council of Kazakhstan, from 2020 to 2023. He is an Associate Editor of IEEE ACCESS and the *Frontiers in Energy Research*.

ARAILYM SERIKBAY (Graduate Student Member, IEEE) received the B.Eng. degree in radio engineering, electronics, and telecommunications from L. N. Gumilyov Eurasian National University, Astana, Kazakhstan, in 2019, and the M.Sc. degree in electrical and computer engineering from Nazarbayev University (NU), Astana, in 2021, where she is currently pursuing the Ph.D. degree in electrical engineering.

From 2020 to 2023, she was a Research Assistant with the Department of Electrical and Computer Engineering, NU. Her research interests include high voltage insulator condition monitoring and assessment, with a specific focus on machine learning.

AMIN ZOLLANVARI (Senior Member, IEEE) received the B.Sc. and M.Sc. degrees in electrical engineering from Shiraz University, Shiraz, Iran, in 2003 and 2006, respectively, and the Ph.D. degree in electrical engineering from Texas A&M University, College Station, TX, USA, in 2010.

He held a postdoctoral position with the Harvard Medical School and the Brigham and Women's Hospital, Boston, MA, USA, from 2010 to 2012, and then he joined the Department of Statistics, Texas A&M University, as an Assistant Research Scientist, from 2012 to 2014. Since 2015, he has been with Nazarbayev University, where he is currently an Associate Professor with the Department of Electrical and Computer Engineering. He has 90 papers in refereed journals and conference proceedings. He is the author of the textbook *Machine Learning with Python: Theory and Implementation* (Springer, 2023). His research interests include machine learning, signal processing, and biomedical informatics.

• • •